Applied Physics Express 7, 112501 (2014)
http://dx.doi.org/10.7567/APEX.7.112501

Suppression of ghost correlation peak in Brillouin optical correlation-domain reflectometry

Neisei Hayashi, Yosuke Mizuno, and Kentaro Nakamura

Precision and Intelligence Laboratory, Tokyo Institute of Technology, Yokohama 226-8503, Japan

Received September 2, 2014; accepted October 14, 2014; published online October 31, 2014

In Brillouin optical correlation-domain reflectometry (BOCDR), an undesired "ghost" correlation peak is automatically generated at the open end of a sensing fiber in addition to the desired correlation peak used for distributed measurement. The Brillouin spectrum of the light scattered from this ghost peak, which has a fixed position, overlaps that from the desired peak, inducing noise and lowering the signal-to-noise ratio. The importance of ghost-peak suppression is experimentally shown by demonstrating that a distributed strain measurement can only be successful when a bending loss of 6 dB or larger is applied near the open end. © 2014 The Japan Society of Applied Physics

Brillouin scattering in optical fibers[1] has been extensively studied for over 40 years and has been applied in the development of several related devices and systems[1–4] including strain and temperature sensors.[5–9] To date, the variety of Brillouin-based distributed sensing techniques that have been demonstrated can be classified into two categories: reflectometry and analysis. In reflectometry, which is based on spontaneous Brillouin scattering, a light beam is injected into only one end of the fiber under test (FUT), whereas in analysis, which is based on stimulated Brillouin scattering, two light beams are injected into both ends of the FUT. Analysis systems include Brillouin optical time-, frequency-, and correlation-domain analysis (BOTDA,[5,10–13] BOFDA,[6,14,15] and BOCDA,[7,16,17] respectively) in which a relatively large signal and high signal-to-noise (SN) ratio can be achieved. However, two-end access is sometimes inconvenient because the system does not work completely when the FUT has a breakage point. Preparation of the probe light often requires relatively expensive devices such as single-sideband modulators, which can be problematic for practical applications. In contrast, even though the signal is weaker, reflectometry systems such as Brillouin optical time- and correlation-domain reflectometry (BOTDR[8,18,19] and BOCDR,[9,20–26] respectively) are free from these drawbacks. Though BOTDR has a measurement range of several tens of kilometers or longer, its spatial resolution is inherently limited to ∼1 m[27,28] even though several methods have recently been developed to enhance the resolution.[10–13,18,19] Thus, we focus on BOCDR in this study.

The BOCDR[9,20–26] operation is based on the so-called "correlation peak"[29] synthesized by the correlation control of two continuous waves (CWs): Brillouin Stokes light and reference light. Furthermore, BOCDR has substantial one-end accessibility, high spatial resolution (13 mm with silica fibers[20] and 6 mm with tellurite fibers[22]), and high sampling rate (i.e., fast measurement speed). One drawback is the trade-off relation between the spatial resolution and the measurement range, which can be mitigated by temporal gating[24] and dual modulation[25] techniques. Another practical merit of BOCDR is the system simplicity, leading to cost efficiency. To further simplify the BOCDR system, we have previously proposed an even simpler implementation of BOCDR, named S-BOCDR,[30] where the light Fresnel-reflected at the open end of the FUT is exploited as the reference light without using the conventional reference path. In S-BOCDR, the zeroth correlation peak is fixed at the FUT end, and the first correlation peak is scanned along the FUT; to avoid spectral overlap and achieve a correct measurement, the influence of the zeroth peak needs to be suppressed either by (1) artificially applying loss near the open end or by (2) cutting the open end at an angle [or by using an angled physical contact (APC)-type connector]. It is notable that a similar situation occurs in the standard BOCDR configuration. To the best of our knowledge, all BOCDR-based distributed measurements along the whole length of the FUT with polarization scrambling (or diversity) have been performed using a specially devised open end [i.e., case (1) or (2)][23] without any specific reason. Note that if the polarization state is optimized for the desired correlation peak, the measurement can sometimes be correctly performed using the open end with a physical contact (PC)-type connector.[9] Further clarification of this point is extremely important for future optimal system design.

In this work, we investigate the influence of this "ghost" correlation peak on BOCDR performance. By measuring the Brillouin spectrum dependence on the bending loss applied near the open end of the FUT, we show that loss greater than 5 dB should be applied to suppress the influence of the ghost peak in this experiment. We also demonstrate a distributed strain measurement with an applied bending loss of 6 dB and present the importance of ghost-peak suppression.

Light propagating in an optical fiber is partially returned via spontaneous Brillouin scattering. The backscattered Stokes light spectrum is called the Brillouin gain spectrum (BGS),[1] and the central frequency of the BGS is shifted downward relative to the incident frequency by an amount termed the Brillouin frequency shift (BFS). The BFS in a standard silica single-mode fiber (SMF) is known to be ∼10.8 GHz at 1.55 μm.[1] If either strain or temperature change is applied to a silica SMF, the BFS shifts toward a higher frequency with dependence coefficients of ∼493 MHz/%[31] and ∼1.0 MHz/K,[32] respectively, at 1.55 μm. Thus, by measuring the BFS, the magnitude of the applied strain or the temperature change can be derived.

To perform a distributed measurement, strain and temperature need to be spatially resolved. The BOCDR is one of the promising Brillouin-based distributed sensing techniques, offering many advantages including one-end accessibility, high spatial resolution, high sampling rate, and cost efficiency. A conceptual schematic of the standard BOCDR setup is depicted in Fig. 1. Its operating principle is based on the correlation control of CWs;[9,21,29] namely, the pump light and the reference light in a standard self-heterodyne scheme for analyzing Brillouin signals[9,33,34] are sinusoidally frequency-modulated at f_m, producing periodic correlation peaks along the FUT. Because only one of these correlation peaks (i.e.,

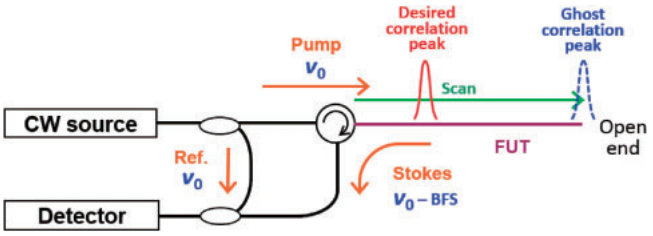

Fig. 1. Conceptual schematic of a standard BOCDR setup for investigating the influence of a ghost correlation peak.

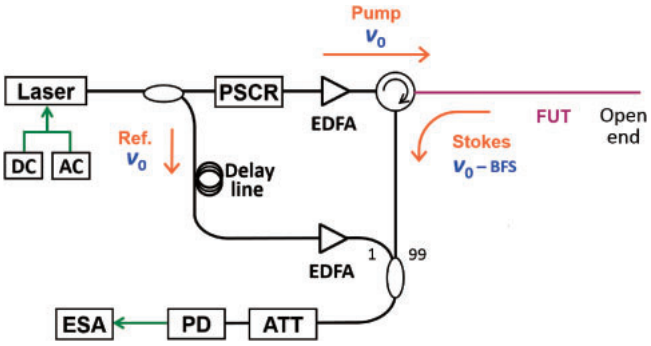

Fig. 2. Experimental setup of a BOCDR system containing an optical attenuator (ATT), EDFAs, an ESA, a PD, and a polarization scrambler (PSCR).

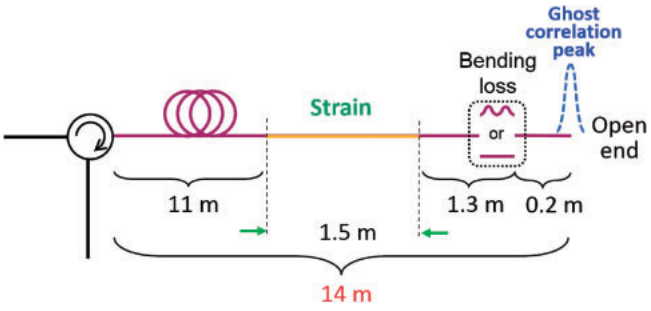

Fig. 3. Structure of the FUT.

sensing positions) should remain in the FUT, the measurement range d_m is determined by their interval, which is inversely proportional to f_m as

$$d_m = \frac{c}{2nf_m}, \quad (1)$$

where c is the velocity of light in vacuum and n is the refractive index of the fiber core. By sweeping f_m, the correlation peak can be scanned along the fiber to acquire the BGS or BFS distribution. When f_m is lower than the Brillouin bandwidth $\Delta\nu_B$ (~30 MHz in a silica SMF[1)]), the spatial resolution Δz is given by[21)]

$$\Delta z = \frac{c\Delta\nu_B}{2\pi n f_m \Delta f}, \quad (2)$$

where Δf is the modulation amplitude of the optical frequency. This is the basic theory regarding BOCDR operation, but we note here that an undesired "ghost" correlation peak exists at the open end of the FUT, as shown in Fig. 1. This peak occurs because the zeroth correlation peak is generally generated at the zero-optical-path-length-difference position, which is the open end of the FUT where the Fresnel-reflected light acts as a reference light (refer to the S-BOCDR scheme[30)] for more details on the zeroth-peak generation). This ghost peak produces a noise source and deteriorates the SN ratio of a distributed measurement because the Brillouin spectrum from the ghost peak constantly overlaps that from the desired peak.

The experimental BOCDR setup for investigating the influence of the ghost correlation peak is shown in Fig. 2. All optical paths were composed of silica SMFs. A distributed-feedback laser diode at 1.55 μm with 1 MHz linewidth was used as a light source, and the optical frequency of its output was sinusoidally modulated by direct modulation of the driving current. The frequency-modulated output was divided into two beams with a 3 dB coupler. One beam was guided through a 1 km delay line to adjust the correlation peak order, amplified to ~22 dBm with an erbium-doped fiber amplifier (EDFA), and used as the reference light of heterodyne detection. The other beam was polarization-scrambled,[23)] amplified with another EDFA, and injected into the FUT as the pump light with an incident power of 28 dBm. A 99:1 coupler was used to mix the Stokes light and the reference light to obtain their optical beat signal, which was attenuated by 12.8 dB, converted to an electrical signal with a photo detector (PD), and finally monitored with an electrical spectrum analyzer (ESA) with 300 kHz frequency resolution. Here, the attenuation was required to avoid gain saturation of the PD output.

For the FUT, we used a silica SMF with a length of 14 m, a numerical aperture of 0.13, a core diameter of 9 μm, a cladding diameter of 125 μm, a core refractive index of ~1.46, and a propagation loss of ~0.5 dB/km at 1.55 μm. The modulation frequency f_m was swept from 2.8557 to 2.9394 MHz, corresponding to the measurement range d_m of 35 m according to Eq. (1). The modulation amplitude Δf was set to 0.7 GHz, resulting in the theoretical spatial resolution Δz of 48 cm from Eq. (2). The fourteenth correlation peak was used. The overall sampling rate of a single-location measurement was ~3.3 Hz; as the number of the sensing points was 280, the total measurement time was ~84 s.

First, we performed a distributed strain measurement without suppressing the ghost correlation peak. The FUT structure is shown in Fig. 3. A strain of 0.20% was applied to a 1.5 m long section of the SMF. The end of the FUT was kept open, meaning a ghost peak exists at the open end. Figure 4 shows the measured BGS distribution along the FUT, where the strained section was not detected.

Next, using the same FUT, we applied a variable bending loss near the open end, as shown in Fig. 3. Figure 5(a) shows the BGS dependence on the bending loss measured when the desired correlation peak was fixed at the midpoint of the strained section. Owing to the scrambled polarization state, the spectral power fluctuations were less than ±0.05 dB. Without the bending loss, the BGS peak was observed at ~10.87 GHz, which corresponds to the BFS of an unstrained silica SMF near the open end, where the ghost peak was fixed (the shape of the peak was slightly distorted because of the noise floor of the ESA[23)]). However, with increasing bending loss, the BGS peak at ~10.87 GHz gradually disappeared. At ~6 dB, a BGS peak at ~10.98 GHz was clearly observed,

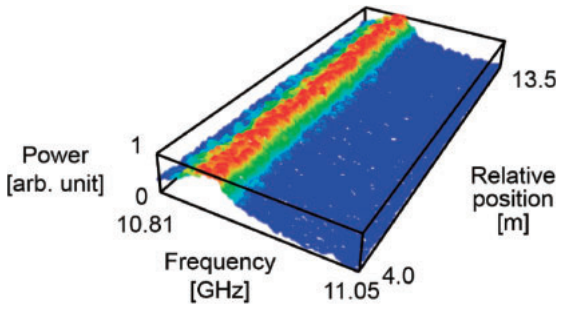

Fig. 4. The BGS distribution measured with an open FUT end. A 0.20% strain was partially applied to the FUT.

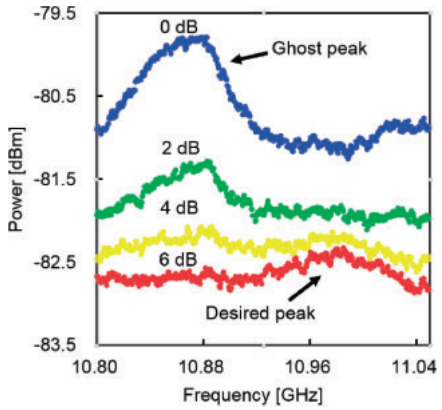

(a)

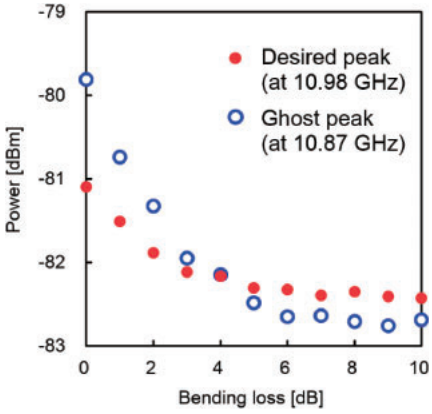

(b)

Fig. 5. (a) BGS dependence on the bending loss measured when the desired correlation peak exists at the midpoint of the strained section (0.20%). (b) BGS peak powers at ~10.98 GHz (desired) and ~10.87 GHz (ghost) measured as functions of bending loss.

which corresponded to the BFS of the strained silica SMF section, where the desired correlation peak existed. Figure 5(b) shows the BGS peak powers at ~10.98 GHz (desired) and ~10.87 GHz (ghost) plotted as functions of the bending loss. As the loss increased, both powers decreased, and the power from the desired peak became higher than that from the ghost peak when the bending loss exceeded approximately 5 dB. This suggests that a loss greater than 5 dB needs to be induced near the open end of the FUT to correctly perform a distributed strain measurement in this configuration.

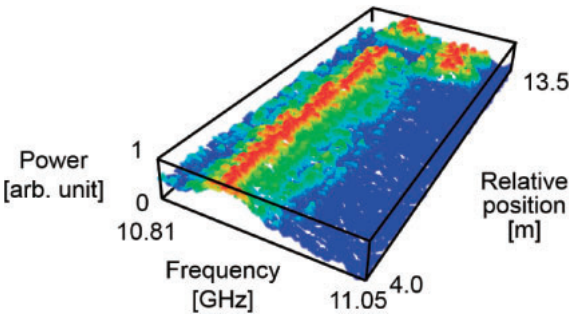

(a)

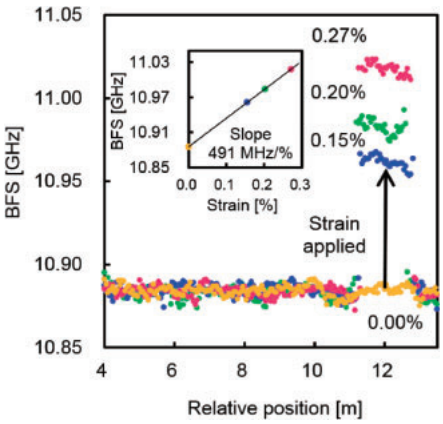

(b)

Fig. 6. (a) BGS distribution measured when a 6 dB bending loss was applied near the FUT end. A 0.20% strain was partially applied to the FUT. (b) BFS distributions measured when the applied strains were 0.15, 0.20, and 0.27%.

Finally, a distributed measurement was performed when 6 dB bending loss was applied near the FUT end. Other experimental conditions were the same as those described above (i.e., those used to obtain Fig. 4). Figure 6(a) shows the BGS distribution measured when the applied strain was 0.20%; the strained section was correctly detected. Note that the SN ratio of this measurement is lower than that of some previously reported results.[9,20,23] This low SN ratio originates from the fact that the optical heterodyne signal was artificially attenuated by 12.8 dB to avoid gain saturation of the PD when the high-power light Fresnel-reflected at the FUT end (without the bending loss) was returned. When a greater than 6 dB bending loss is applied, this attenuator can be removed, leading to a drastic enhancement of the SN ratio. Figure 6(b) shows the BFS distributions measured when the applied strains were 0.15, 0.20, and 0.27%. As shown in the inset, the BFS was linearly dependent on the applied strain with a proportionality coefficient of ~491 MHz/%, which is in good agreement with the previous report.[31] Thus, we clarified that the ghost peak must be sufficiently suppressed to correctly perform distributed measurements using BOCDR.

In conclusion, the influence of the ghost correlation peak on the BOCDR performance was experimentally investigated. First, a correct distributed strain measurement was shown to be infeasible if the FUT end was simply kept open. The BGS dependence on the bending loss applied near the open end to suppress the ghost peak was also measured, and a loss greater than 5 dB was required. A successful distributed

strain measurement was then demonstrated when the ghost peak was sufficiently suppressed. From these results, ghost-peak suppression was shown to be crucial for correct BOCDR operation. Theoretically, the value of 5 dB is almost independent of the FUT length or the spatial resolution (or measurement range). The former case occurs because the propagation loss of the SMF is as small as ~0.5 dB/km (note that, in BOCDR, an FUT with a length of several tens of kilometers is seldom used because it results in quite poor spatial resolution (greater than several meters) owing to the resolution/range trade-off relation). The latter case occurs because the resolution affects only the width of the correlation peak. If the resolution is extremely low, the position of the bending loss needs to be farther from the FUT end. In particular, the following criterion can be used for determining the position at which bending loss should be applied, i.e., the loss should be applied at a position that is approximately half of the spatial resolution far from the FUT open end (as in this experiment). Though bending loss was used in this work, cutting the FUT end at an angle or using an APC-type connector at the FUT end could be an alternative method. Our results also suggest that the FUT should not contain reflective spots such as badly coupled or spliced points and inherent fiber defects because another ghost peak may be generated. We believe that this study will provide a useful guideline for optimal BOCDR system design in the future.

Acknowledgments This work was partially supported by Grants-in-Aid for Young Scientists (A) (No. 25709032) and for Challenging Exploratory Research (No. 26630180) from the Japan Society for the Promotion of Science (JSPS) and by research grants from the General Sekiyu Foundation, the Iwatani Naoji Foundation, and the SCAT Foundation. N.H. acknowledges a Grant-in-Aid for JSPS Fellows (No. 25007652).

1) G. P. Agrawal, *Nonlinear Fiber Optics* (Academic Press, San Diego, CA, 1995).
2) S. Norcia, S. Tonda-Goldstein, D. Dolfi, and J. P. Huignard, Opt. Lett. **28**, 1888 (2003).
3) Z. Zhu, D. J. Gauthier, and R. W. Boyd, Science **318**, 1748 (2007).
4) K. Y. Song, M. G. Herraez, and L. Thevenaz, Opt. Express **13**, 82 (2005).
5) T. Horiguchi and M. Tateda, J. Lightwave Technol. **7**, 1170 (1989).
6) D. Garus, K. Krebber, and F. Schliep, Opt. Lett. **21**, 1402 (1996).
7) K. Hotate and T. Hasegawa, IEICE Trans. Electron. **E83-C**, 405 (2000).
8) T. Kurashima, T. Horiguchi, H. Izumita, and M. Tateda, IEICE Trans. Commun. **E76-B**, 382 (1993).
9) Y. Mizuno, W. Zou, Z. He, and K. Hotate, Opt. Express **16**, 12148 (2008).
10) K. Y. Song and H. J. Yoon, Opt. Lett. **35**, 52 (2010).
11) T. Sperber, A. Eyal, M. Tur, and L. Thevenaz, Opt. Express **18**, 8671 (2010).
12) Y. Dong, H. Zhang, L. Chen, and X. Bao, Appl. Opt. **51**, 1229 (2012).
13) Y. Mao, N. Guo, K. L. Yu, H. Y. Tam, and C. Lu, IEEE Photonics J. **4**, 2243 (2012).
14) A. Minardo, R. Bernini, and L. Zeni, IEEE Photonics Technol. Lett. **26**, 387 (2014).
15) A. Wosniok, Y. Mizuno, K. Krebber, and K. Nakamura, Proc. SPIE **8794**, 879431 (2013).
16) K. Y. Song, Z. He, and K. Hotate, Opt. Lett. **31**, 2526 (2006).
17) J. H. Jeong, K. H. Chung, S. B. Lee, K. Y. Song, J.-M. Jeong, and K. Lee, Opt. Express **22**, 1467 (2014).
18) M. A. Soto, G. Bolognini, and F. D. Pasquale, IEEE Photonics Technol. Lett. **21**, 450 (2009).
19) F. Wang, W. Zhan, X. Zhang, and Y. Lu, J. Lightwave Technol. **31**, 3663 (2013).
20) Y. Mizuno, Z. He, and K. Hotate, IEEE Photonics Technol. Lett. **21**, 474 (2009).
21) Y. Mizuno, W. Zou, Z. He, and K. Hotate, J. Lightwave Technol. **28**, 3300 (2010).
22) Y. Mizuno, Z. He, and K. Hotate, Opt. Commun. **283**, 2438 (2010).
23) Y. Mizuno, Z. He, and K. Hotate, Appl. Phys. Express **2**, 062403 (2009).
24) Y. Mizuno, Z. He, and K. Hotate, Opt. Express **17**, 9040 (2009).
25) Y. Mizuno, Z. He, and K. Hotate, Opt. Express **18**, 5926 (2010).
26) N. Hayashi, Y. Mizuno, and K. Nakamura, J. Lightwave Technol. **32**, 3397 (2014).
27) A. Fellay, L. Thevenez, M. Facchini, M. Nikles, and P. Robert, Tech. Dig. Opt. Fiber Sens. **16**, 324 (1997).
28) H. Naruse and M. Tateda, Appl. Opt. **38**, 6516 (1999).
29) K. Hotate, Meas. Sci. Technol. **13**, 1746 (2002).
30) N. Hayashi, Y. Mizuno, and K. Nakamura, IEEE Photonics J. **6**, 6802807 (2014).
31) T. Horiguchi, T. Kurashima, and M. Tateda, IEEE Photonics Technol. Lett. **1**, 107 (1989).
32) T. Kurashima, T. Horiguchi, and M. Tateda, Appl. Opt. **29**, 2219 (1990).
33) Y. Mizuno and K. Nakamura, Appl. Phys. Lett. **97**, 021103 (2010).
34) Y. Mizuno and K. Nakamura, Opt. Lett. **35**, 3985 (2010).